Pergamon

0301-9322(94)E0032-E

Int. J. Multiphase Flow Vol. 20, No. 4, pp. 721–737, 1994
Elsevier Science Ltd. Printed in Great Britain

ON DENSITY-WAVE OSCILLATIONS IN TWO-PHASE FLOWS

RIZWAN-UDDIN

Department of Mechanical, Aerospace and Nuclear Engineering, University of Virginia, Charlottesville, VA 22903-2442, U.S.A.

(Received 30 August 1993; in revised form 6 April 1994)

Abstract—Density-wave oscillations in two-phase boiling flow systems have been studied numerically using a robust model based on two non-linear, functional, integro-differential equations. Results of several numerical simulations are used to gain insight into the physical mechanism behind density-wave oscillations. For a wide range of parameter values we find that: (1) traveling density-waves do not play an important role during the oscillations, and that oscillations may persist with very weak traveling density waves; (2) the oscillation period is between three and four times the channel transit time rather than twice as commonly reported; and (3) the variation in mixture velocity, in general, plays a more important role than the variation in mixture density in determining the channel pressure drop characteristics. A physical mechanism for these non-linear oscillations applicable to a large region of parameter space, as suggested by—and consistent with—the results of the numerical experiments, is proposed.

Key Words: density-wave oscillations, two-phase flow, numerical analysis

INTRODUCTION

Density-wave oscillations in heated channels (Stenning & Veziroğlu 1965) have been studied extensively over the last three decades. These oscillations have been reviewed periodically (Bouré *et al.* 1973; Lahey & Moody 1977; Bouré 1978; Bergles 1981; Kakaç & Liu 1991). A typical heated channel with single- and two-phase flow is shown schematically in figure 1. Flow is due to an externally imposed pressure drop, ΔP_{ex}, and the fluid at the channel inlet is, in general, subcooled. Heat added along the channel length causes the flowing liquid to boil. Axial location at which boiling starts is denoted by λ, the boiling boundary. A mixture of liquid and vapor leaves the channel at the exit. System operating parameters are imposed pressure drop, inlet temperature and total heat supplied. Under certain conditions, steady-state solution of such two-phase boiling flow systems becomes unstable, resulting in oscillations with frequency in the order of 0.1–1 Hz. Oscillation amplitude usually saturates at an asymptotic value. Bifurcation analyses of these so-called density-wave oscillations show that, as one or more system parameters are varied across the stability boundary, supercritical Hopf bifurcation occurs (Hopf 1942; Hassard *et al.* 1981), resulting in stable limit cycle solutions to which the system evolves (Achard *et al.* 1985; Rizwan-uddin & Dorning 1986; Rizwan-uddin 1986). Comparison of the results of the bifurcation analysis has shown good agreement with experimental data (Rizwan-uddin & Dorning 1986).

The physical mechanism of self-sustained density-wave oscillations in heated channels with two-phase boiling flow has been explained in various ways in the past (Stenning & Veziroğlu 1965; Bouré *et al.* 1973; Lahey & Moody 1977; Bouré 1978; Bergles 1981; Kakaç & Liu 1991). One approach, which relies on the simplified concentrated pressure drop model, is based on following the effect of an instantaneous, say positive, perturbation in inlet velocity (flow rate) that transforms into a *wave* of higher density in the two-phase region, and causes the exit pressure drop to increase at a later time when the higher density wave reaches the channel exit. Hence, in order to keep the total pressure drop at a constant value specified as the boundary condition, there results an instantaneous *drop* in the inlet velocity. The process is reversed as the density wave, resulting from the lower inlet velocity, travels to the channel exit: the pressure drop at the channel exit decreases as the wave of lower density reaches the top, resulting in an increase in the inlet flow rate, and starting the cycle over again. This approach describes the oscillations as the product of enthalpy

perturbations which travel with mixture flow velocity, and result in fluid waves of alternatively higher and lower density mixture *traveling across the system* (Kakaç & Liu 1991). According to this description, the *traveling density waves*—which affect the pressure drop in the channel in such a way that self-sustained oscillations result—appear to be an important characteristic of these oscillations. Moreover, based on these descriptions, the period of oscillation is generally reported to be about *one to two times* the transit time through the channel (Bouré 1978). Though relevant for some cases, we find that in large regions of parameter space, the associated changes in mixture *velocity*, by affecting the pressure drop, play as important, and sometimes more important, a role during the oscillation, as variations in mixture density. Detailed analysis of the flow kinetics reported here, shows that for a wide range of parameter values, traveling density waves are not fundamental to the oscillation mechanism. Based on the analytical and numerical results, it is further shown that for these regions in parameter space, the physical description of these oscillations suggests the period to be actually between three to four times the transit time through the channel. This is also strongly supported by data reported in literature.

These non-linear oscillations also have been explained by assuming that inlet perturbations acquire a 180° out-of-phase pressure fluctuation at the exit, which is immediately transmitted to the inlet and results in self-sustained oscillations. Though applicable to oscillations of infinitesimal amplitude, as non-linear a phenomenon as self-sustained oscillations of finite amplitude in heated channels with two-phase flow does not always result in oscillations that are perfectly symmetric and hence, the explanation that inlet flow rate perturbation results in a 180° out-of-phase pressure fluctuation at the exit to cause self-sustained oscillations, must be modified and extended to explain finite amplitude oscillations. Moreover, it is not accurate to associate the pressure fluctuation at the exit during self-sustained oscillations, with a particular perturbation at the channel inlet at some earlier time $(t - a)$. The exit pressure is actually a function of the instantaneous distribution of the kinetic variables *throughout* the channel which are not only a function of the perturbation at time $(t - a)$ but also depend upon the inlet flow rate over the entire interval $(t - a)$ to t. Any explanation of these non-linear oscillations must take into account the flow kinetics—variation of the mixture density and mixture velocity during oscillations, and continuous propagation of the inlet flow variation down stream through the single-phase and the two-phase regions.

In view of the inadequate description of the physical mechanism of the finite amplitude density-wave oscillations, there is a need to analyze these instabilities in more detail. Mathematical

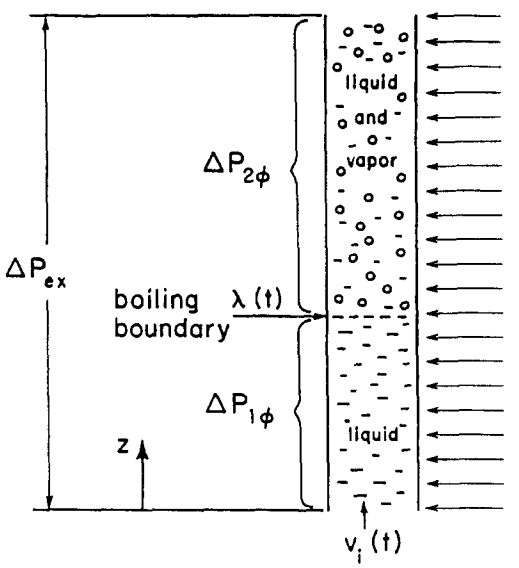

Figure 1. Schematic diagram of a heated channel with single-phase $(0 < z < \lambda)$ and two-phase $(\lambda < z < 1)$ regions. Externally imposed pressure drop is ΔP_{ex} and heat flux is q''.

models used to analyze these oscillations numerically should: (1) capture the underlying dynamics relatively accurately; (2) easily decouple various competing dynamical effects in the channel during the oscillations; and (3) be solvable numerically to simulate finite amplitude oscillations. In this paper, the physical mechanism behind density-wave oscillations is analyzed and explained using a continuous mathematical model. This model is particularly useful—as it allows reconstruction of the time-dependent and space-and-time-dependent variables in the channel during constant amplitude oscillations—in extracting the details in the variation of pressure drop components, and to study how individual components affect the flow rate and lead to constant amplitude oscillations. It has been used previously for the stability and bifurcation analysis of these non-linear oscillations (Achard *et al.* 1985; Rizwan-uddin & Dorning 1986). The set of equations in this model was linearized about a fixed point (equilibrium or steady-state) and solved for analytical stability studies of the system, and the stability boundary in parameter space was determined. Then the Hopf bifurcation that occurs as the parameters are moved across the stability boundary was studied using the Lindstedt–Poincaré technique. It was thus determined that the Hopf bifurcation is supercritical for most cases of practical interest and that there are regions in three-dimensional operating parameter space beyond the stability boundary where stable oscillations exist, i.e. the stable fixed point bifurcates into an unstable fixed point and a stable limit cycle as the boundary is crossed (Achard *et al.* 1985; Rizwan-uddin & Dorning 1986). These analytical studies were carried out for the homogeneous equilibrium model (Achard *et al.* 1985) used here, and also for the more general drift flux model (Rizwan-uddin & Dorning 1986) for two-phase flow. Results for stability boundaries were compared with experimental data and it was found that though the drift flux model improved the agreement between analytical stability boundary and experimental data points, homogeneous equilibrium model also yielded very good agreement. Results of calculations based on both the homogeneous equilibrium model and drift flux model were in good agreement with the results obtained by using the two-fluids model as reported by Dykhuizen *et al.* (1986a). Having compared the results obtained using both the drift flux model and the homogeneous equilibrium model, it is clear that the added effort needed does not warrant the numerical analysis using the drift flux-based model.

MODEL

A two integro-differential equations model is used to study the dynamics of two-phase flow in a heated channel with spatially uniform heat flux. This model was developed—assuming incompressible single-phase flow, and using the homogeneous equilibrium model to represent the two-phase flow (Achard *et al.* 1985; Frutera 1986)—by first integrating the partial differential equations along the characteristics to find the kinetic variables as a function of inlet velocity, substituting the expressions for kinetic variables into the momentum equation and then integrating the momentum equation along the channel length to obtain the total pressure drop equation. The two independent variables in this model are the channel inlet velocity and "two-phase residence time", which is defined as the time spent in the two-phase region by the fluid at the channel exit at time t. This variable is introduced in the analysis while solving the two-phase region mixture density equation (or void propagation equation) using the method of characteristics (Achard *et al.* 1985; Rizwan-uddin & Dorning 1986; Rizwan-uddin 1986). All other dependent variables in the original set of partial differential equations, can be recovered (using exact expressions) once the time evolution of inlet velocity and two-phase residence time has been determined. The homogeneous equilibrium model has been used for three reasons: (1) frequency domain stability analyses show that this model is quite capable of predicting the onset of instability (Rizwan-uddin & Dorning 1986); (2) constitutive relationship for a time-dependent drift flux model-based analysis, and constitutive relationships for momentum and energy transfer between phases, between phases and channel wall, and the flow regime diagram, necessary for a time-dependent two-fluid model based analysis, are still not accurately known; and (3) numerical analysis of the two integro-differential equations-based model used here, is significantly more robust and efficient compared to analyses that use models based on partial differential equations.

The single-phase and two-phase flow equations are made dimensionless using the dimensionless variables and parameters given in the appendix (Achard *et al.* 1985; Rizwan-uddin & Dorning 1986). The equation for the total pressure drop is

$$\Delta P_{\text{tot}} = \Delta P_{\text{i}} + \Delta P_{1\phi} + \Delta P_{2\phi} + \Delta P_{\text{e}} = \Delta P_{\text{ex}} \tag{1}$$

where the subscripts tot, i, 1ϕ, 2ϕ, e and ex denote total, inlet, single-phase, two-phase, exit and external, respectively. Externally imposed pressure drop ΔP_{ex}, is specified as boundary condition, and ΔP_{i}, ΔP_{e} depend upon kinetic variables, and are given by

$$\Delta P_{\text{i}}(t) = k_{\text{i}} v_{\text{i}}^2(t) \tag{2}$$

and

$$\Delta P_{\text{e}}(t) = k_{\text{e}} \rho_{\text{m}}(z = 1, t) j^2(z = 1, t) \tag{3}$$

where k_{i} and k_{e} are inlet and exit restriction coefficient, v_{i} is the inlet velocity and $\rho_{\text{m}}(z, t)$ and $j(z, t)$ are mixture density and volumetric flux (or mixture velocity), respectively. Single-phase and two-phase region pressure drops are obtained by first integrating along the characteristics for kinetic variables, and then after substituting the kinetic variables, integrating the single- and two-phase momentum equations along their respective single- and two-phase region lengths for pressure drop (Achard *et al.* 1985; Rizwan-uddin & Dorning 1986),

$$\Delta P_{1\phi}(t) = \underbrace{\left[\frac{\mathrm{d}v_{\text{i}}(t)}{\mathrm{d}t}\right]}_{\text{inertia}} + \underbrace{N_{\text{fl}} v_{\text{i}}^2(t)}_{\text{friction}} + \underbrace{\mathrm{Fr}^{-1}}_{\text{gravity}} \lambda(t) \tag{4}$$

$$\begin{aligned}
\Delta P_{2\phi}(t) = {} & J_1(t)\frac{\mathrm{d}v_{\text{i}}(t)}{\mathrm{d}t} + && \text{(inertia)} \\
& N_{\text{pch}}[v_{\text{i}}(t - v)J_1(t) + N_{\text{pch}} J_2(t)] + && \text{(convection)} \\
& N_{\text{f2}}[v_{\text{i}}^2(t)J_1(t) + 2N_{\text{pch}} v_{\text{i}}(t)J_2(t) + N_{\text{pch}}^2 J_3(t) + && \text{(friction)} \\
& \mathrm{Fr}^{-1} J_1(t) && \text{(gravity)}
\end{aligned} \tag{5}$$

where the boiling boundary, $\lambda(t)$—defined as the axial location at which bulk fluid temperature reaches the saturation temperature (Achard *et al.* 1985)—is obtained by solving the single-phase energy equation, and is given by

$$\lambda(t) = \int_{t-v}^{t} v_{\text{i}}(\sigma)\mathrm{d}\sigma, \tag{6}$$

$\tau_{2\phi}(t)$ is the two-phase residence time, given by

$$1 - \lambda(t) = \int_0^{\tau_{2\phi}(t)} \mathrm{e}^{N_{\text{pch}}\sigma} v_{\text{i}}(t - v - \sigma)\mathrm{d}\sigma, \tag{7}$$

$J_1(t)$, $J_2(t)$, $J_3(t)$ and $J_4(t)$ are given by

$$J_1(t) \equiv \int_0^{\tau_{2\phi}(t)} v_{\text{i}}(t - \sigma - v)\mathrm{d}\sigma \tag{8}$$

$$J_2(t) \equiv \int_0^{\tau_{2\phi}(t)} v_{\text{i}}(t - \sigma - v)\mathrm{d}\sigma \int_0^{\sigma} \mathrm{e}^{N_{\text{pch}}\eta} v_{\text{i}}(t - \eta - v)\mathrm{d}\eta \tag{9}$$

$$J_3(t) \equiv \int_0^{\tau_{2\phi}(t)} v_{\text{i}}(t - \sigma - v)\mathrm{d}\sigma \left[\int_0^{\sigma} \mathrm{e}^{N_{\text{pch}}\eta} v_{\text{i}}(t - \eta - v)\mathrm{d}\eta\right]^2 \tag{10}$$

$$J_4(t) \equiv \int_0^{\tau_{2\phi}(t)} \mathrm{e}^{N_{\text{pch}}\sigma} v_{\text{i}}(t - \sigma - v)\mathrm{d}\sigma \tag{11}$$

and single-phase residence time v is given by

$$v \equiv \frac{N_{sub}}{N_{pch}}.$$

The dimensionless parameters N_{sub}, N_{pch}, N_{f1} and N_{f2} are proportional to inlet subcooling, total heat supplied, single-phase friction and two-phase friction, respectively. Substituting [2–5] in [1] yields the second integro-differential equation for the channel dynamics

$$\frac{dv_i(t)}{dt} = \frac{1}{(\lambda(t) + J_1(t))}\Big\{ -k_i v_i^2(t) - k_e e^{-N_{pch}\tau_{2\phi}(t)}[v_i(t) + N_{pch}J_4(t)]^2 - N_{f1}v_i^2(t)\lambda(t) - Fr^{-1}(\lambda(t) + J_1(t)) - N_{pch}v_i(t-v)J_1(t) - N_{pch}^2 J_2(t) - N_{f2}[v_i^2(t)J_1(t) + 2N_{pch}v_i(t)J_2(t) + N_{pch}^2 J_3(t)] + \Delta P_{ex}(t)\Big\} \quad [12]$$

where $\tau_{2\phi}(t)$ is given by [7].

Equations [7] and [12] can be solved using standard numerical techniques (Rizwan-uddin & Dorning 1990). The time- and space-and-time-dependent variables in the channel can be easily reconstructed once [7] and [12] have been solved for $v_i(t)$ and $\tau_{2\phi}(t)$. In the single-phase region, which extends up to $\lambda(t)$, the (dimensionless) density is one, and the flow velocity is equal to the channel inlet velocity (incompressible liquid). In the two-phase region, the mixture velocity or volumetric flux $j(z, t)$ is given by

$$j(z, t) = v_i(t) + N_{pch}(z - \lambda(t)) \quad [13]$$

and mixture density $\rho_m(z, t)$ is given by

$$\rho_m(z, t) = e^{-N_{pch}\sigma(z)} \quad [14]$$

where σ and z are related by

$$z = \lambda(t) + \int_0^{\sigma} e^{N_{pch}\eta} v_i(t - v - \eta)d\eta \quad [15]$$

Note, σ is actually the time interval that the fluid particle at $z(t)$ ($z \geqslant \lambda(t)$) has spent in the two-phase region (Achard *et al.* 1985). An important variable in the analysis that follows is the total "channel residence time," which is the sum of the single-phase residence time v, and the two-phase residence time $\tau_{2\phi}$. Single-phase residence time at steady-state and for the case of uniform axial heat flux, even during transients, is constant and is given by N_{sub}/N_{pch} (Achard *et al.* 1985; Rizwan-uddin & Dorning 1986). Two-phase residence time at steady-state $\tilde{\tau}_{2\phi}$ is given by $\ln[1 + (N_{pch}/\tilde{v} - N_{sub})]/N_{pch}$, and during the oscillations it is actually one of the dependent variables calculated using [7] and [12].

The model described above ([7] and [12]) can easily be solved for different parameter values. The numerical scheme used to solve the non-linear integro-differential equations has been described earlier (Rizwan-uddin & Dorning 1990). The derivative in [12] was approximated by fully implicit backward difference with second-order global error. However, the set of non-linear integro-differential equations cannot be integrated directly due to the history integrals $J_i(t)$ ($i = 1, \ldots, 4$) that appear in them. The two-phase residence time $\tau_{2\phi}(t)$ appears as the upper limits of these integrations backwards in time. Thus, although the integrals only have to be carried out over past times where the values of $v_i(t)$ already have been calculated and the starting point of the integration interval is known, the end of this interval is not known *a priori*. Hence, the discretized forms of the equations, starting from predicted values for $v_i(t_j)$ and $\tau_{2\phi}(t_j)$ at each time step t_j, were solved iteratively using a second-order Newton method. The iterations always converged rapidly even though the non-linear equations are transcendental in $\tau_{2\phi}(t_j)$. The integrands of the integrals $\lambda(t)$ and $J_i(t)$ ($i = 1, \ldots, 4$) in the interiors of the time intervals Δt_j were approximated linearly in terms of the values at the edges, and the integrals were then evaluated via a trapezoidal rule leading to second-order global error in Δt_j. Hence, the truncation error in the approximate evaluation of the

integrals was consistent with the backward differencing of the derivatives, and the numerical scheme used has second-order global error (Rizwan-uddin & Dorning 1990).

Constant time steps Δt were generally used except at the end points of the history integrals being evaluated, which, due to the variable integration interval, sometimes required a time step $< \Delta t$ (at the ends of the integration interval). The size of the dimensionless time step Δt was varied to ensure the results were converged as a function of Δt. The value used to obtain all the results reported here was $\Delta t = 0.01$, which is much smaller than all oscillation time scales studied.

The model described above very conveniently yields various pressure drop components that constitute the total channel pressure drop. Limit cycle solutions for increasingly more detailed models are obtained, time- and space-and-time-dependent variables are reconstructed and plotted over one period of (stable) oscillation cycle for these cases. A detailed analysis of these plots reveals several interesting features of the mechanism behind the non-linear oscillations.

ANALYSIS AND RESULTS

Understanding the physical mechanism behind density-wave oscillations, requires understanding of the operating feedback mechanism and the heated channel kinetics. The feedback mechanism is discussed first.

For constant channel inlet temperature, the feedback mechanism during the oscillation directly affects the inlet velocity (or inlet flow rate). The other dependent variables change as a result of their dependence upon the inlet velocity. Hence, during the oscillation, the inlet velocity immediately responds to changes in various pressure drop components, and then the variations in inlet velocity, as they are propagated through the single- and two-phase regions, affect the other dependent variables, such as the pressure drop components. The underlying mechanism for the change in inlet velocity, for the case of constant externally imposed pressure drop, is rather simple: inlet velocity evolves to keep the total internal pressure drop constant. For example, consider a heated channel with pressure drops concentrated at the inlet and exit, i.e. total pressure drop is the sum of concentrated pressure drops at the channel inlet and exit. Moreover, if the pressure drop at the exit at time t is only a weak function of inlet velocity (at time t), then an increase in exit pressure drop, possibly due to a perturbation, would—to keep the total pressure drop constant—require a decrease in inlet pressure drop via a decrease in inlet velocity.

Channel internal pressure drop at any time t depends upon the instantaneous distribution of kinetic variables (boiling boundary, mixture velocity, mixture density), which in turn depend upon the inlet flow rate during a finite interval $(t - a)$ to t. Hence, to determine the delayed effect of inlet velocity variation on pressure drop characteristic, the evolution of kinetic variables as a function of inlet velocity variation must first be determined. For example, as stated before, distributed pressure drop in the two-phase region and concentrated pressure drop at the exit are not only a function of mixture density, but also depend upon volumetric flux (or mixture velocity). Hence, to determine the physical process behind the oscillations, knowledge of time variations of both of these space-dependent variables [$\rho_m(z, t)$ and $j(z, t)$] is necessary. Time variation of the individual pressure drop components such as single-phase region pressure drop, two-phase region pressure drop, inlet restriction pressure drop and exit restriction pressure drop, along with time variation of the inlet flow rate and boiling boundary at the periodically oscillating state, will significantly help in identifying the feedback process that results in constant amplitude oscillations.

A simple heated channel with the pressure drop concentrated at the channel inlet and channel exit is analyzed first as case A. This model is used to identify characteristic trends during stable oscillations, and to develop the underlying mechanism behind these non-linear oscillations. The physical relationship between oscillation period and channel transit time is also explained, using this model. Differences between characteristics observed here and those reported earlier are pointed out. A more general model that includes distributed pressure drop in the single-phase and two-phase regions is studied next as case B. Based on the numerical results obtained for these two cases, the physical mechanism behind constant amplitude oscillations is explained. The effect on stability of higher fractional pressure drop near the exit is explicitly studied using a numerical example.

Table 1

Parameters	N_{sub}	10.00
	N_{pch}	16.85
	ΔP_{ex}	22.1244
	Fr^{-1}	0.0
	N_{fl}	0.0
	N_{fl2}	0.0
	k_i	6.00
	k_e	2.05
Dependent variables	Inlet velocity	1.000
	Boiling boundary	0.5935
	ΔP_i	6.00
	ΔP_e	16.1244
	$\Delta P_{1\phi}$	0.0
	$\Delta P_{2\phi}$	0.0
	$\Delta P_{tot}(=\Delta P_{ex})$	22.1244

Case A

Although the more general problem, in which distributed pressure drop in the single-phase and two-phase regions is included, is investigated next, since the channel with pressure drop concentrated at the channel inlet and exit has traditionally been used to explain these oscillations (Friedly & Krishnan 1972), analysis of a simplified heated channel with pressure drop concentrated at the channel inlet and at the channel exit is carried out first for comparison purposes. Equation [1] for this case reduces to

$$\Delta P_{ex} = \Delta P_i(t) + \Delta P_e(t) = \text{constant} \qquad [16]$$

where $\Delta P_i(t)$ and $\Delta P_e(t)$ are given by [2] and [3]. The parameter values used, and selected dependent variables at the (unstable) steady-state for this problem (case A), are given in table 1. As a perturbation is introduced in the inlet velocity at time $t = 0$, the inlet flow rate, and all other dependent variables, gradually evolve from the unstable steady-state solution (or unstable fixed point) to limit cycle oscillations. The evolution of the inlet velocity is shown in figure 2(a). Figure 2(b) shows the trajectory in a projection of the phase space onto the two-dimensional v_i–λ plane. To determine the oscillation mechanism at the *constant amplitude oscillation*, in figure 3, the variation of the dependent variables over one period of stable oscillation is plotted. In figure 3(a)–(e) are shown the inlet and exit pressure drop, inlet velocity, boiling boundary, mixture density and mixture velocity at four points in the two-phase region ($z = 0.75$, 0.8, 0.9, 1.0), and channel residence time. Also shown in this figure are dashed vertical lines (A–H) to guide the eye. The inlet velocity is at the unstable steady-state value of 1.0 at times A and E. It is at its minimum and maximum at times C and G, respectively. Inlet velocity is half way between minimum and 1.0 at times B and D, and half way between maximum and 1.0 at times F and H. The following observations can be made:

(1) The exit pressure drop oscillation and the oscillation in the mixture density at the exit are out of phase: though the exit mixture density is decreasing between times H–A–B–C, the exit pressure drop is increasing. This increase is due to the increase in exit volumetric flux. Clearly, since the pressure drop at the exit—which is a function of (proportional to) density and velocity at the exit—is varying in-phase with the velocity and out-of-phase with mixture density, the former must play a more dominant role than the latter.
(2) The period of oscillation is 2.4, where as the channel transit time oscillates between 0.68 and 0.74. (While the single-phase residence time is equal to $\nu \equiv N_{sub}/N_{pch} = 0.59$, two-phase residence time actually oscillates.) Note the oscillation period is significantly larger than twice (almost four times) the average transit time through the channel.
(3) Mixture density at $z = 0.7$, 0.8, 0.9 and 1.0 reaches maxima at about the same time, indicating an almost simultaneous increase and decrease of mixture density in the entire two-phase region, with a rather weak traveling wave riding on top of the steady-state solution from the lower end of the two-phase region to the top.

It is clear that the observations stated above do not support the traditional explanations of the physical mechanism behind density-wave oscillations. Specifically, the pressure drop characteristics within the channel is influenced more strongly by the mixture velocity (volumetric flux) than by mixture density; the oscillation period is closer to four times the channel transit time, rather than twice; and the traveling density waves—that are, in classical explanations, an important characteristic of such oscillations—appear to be very weak. It should also be noted that during stable oscillations, increase in inlet velocity oscillation amplitude occurs over 41% of the oscillation period and the amplitude decreases over the remaining 59% of the period. These oscillations are clearly not a result of perturbations acquiring a 180° out-of-phase pressure fluctuation at the exit.

A detailed explanation of the numerical results presented in figures 2 and 3 is given below in two subsections, analyzing (1) the importance of mixture density versus mixture velocity and the role of density waves and (2) the relationship between the oscillation period and channel residence time. Note, all variables are dimensionless, the steady-state value of the inlet velocity is 1.0, and at the stable limit cycle the inlet velocity oscillates with an amplitude of approx. 0.24.

Mixture density versus mixture velocity

To establish the relative importance of mixture density variation versus mixture velocity variation during the oscillations, changes in the two variables and their effects on total pressure

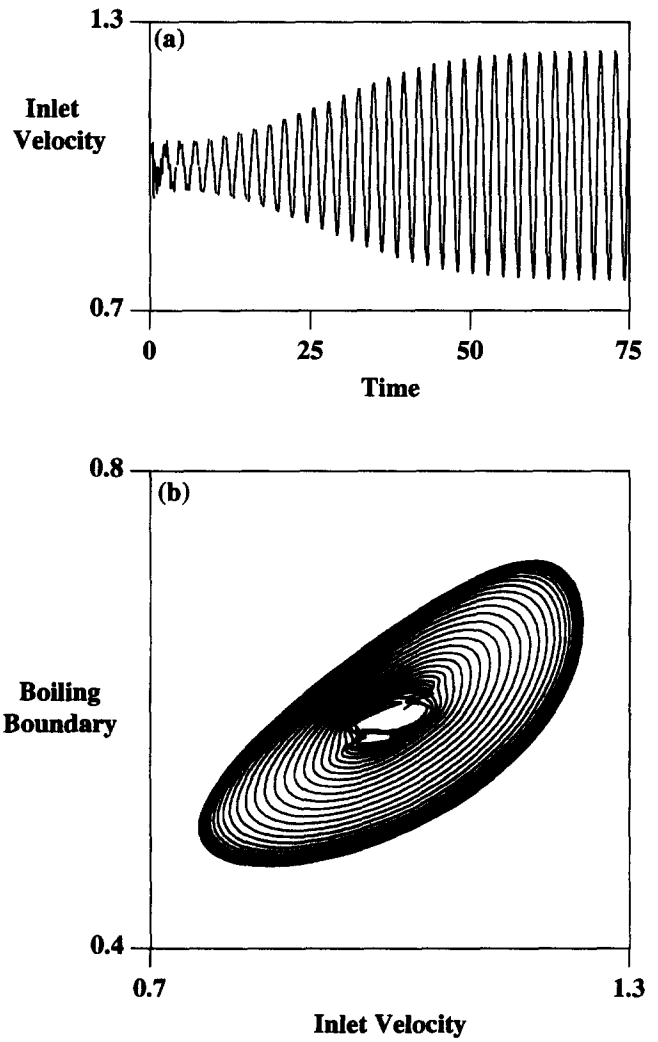

Figure 2. (a) Evolution of the inlet velocity as a function of time for case A. (b) Trajectory in a projection of the phase space onto the two-dimensional v_i–λ plane.

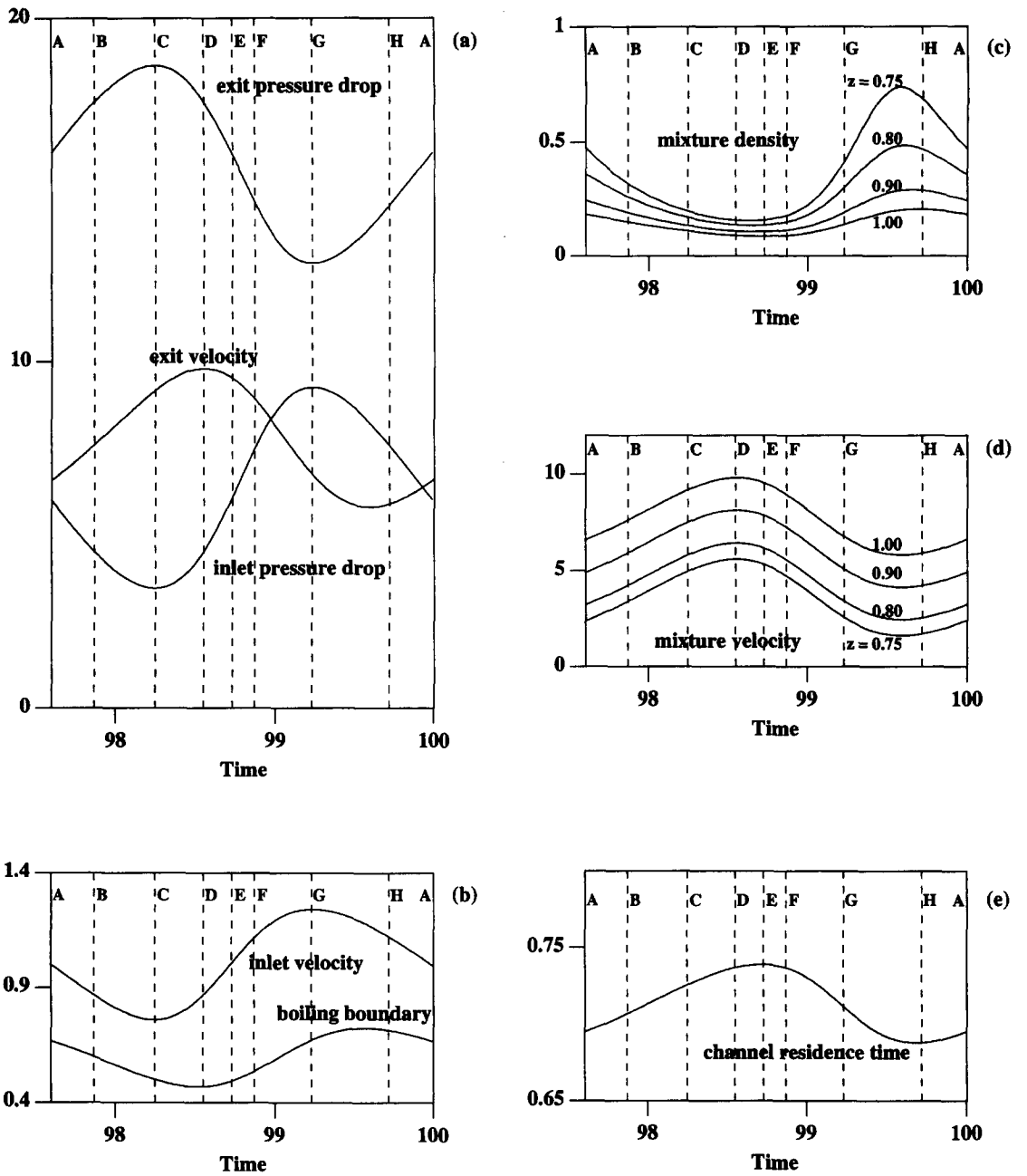

Figure 3. (a–e) Variation of the dependent variables over one period of the stable oscillation for case A. Shown are, inlet and exit pressure drop, inlet velocity, boiling boundary, mixture density and mixture velocity at four points in the two-phase region ($z = 0.75$, 0.8, 0.9, 1.0), and channel residence time ($v + \tau_{2\phi}$).

drop in the channel are analyzed by following their evolution, assuming that the inlet velocity is specified, and the other dependent variables actually follow from it. We start at time C, where the inlet velocity is at its minimum and starts to rise. First, note that the boiling boundary responds to the increase in inlet velocity that starts at C with a certain delay and only starts to move up after $\Delta t \simeq 0.3$ (dimensionless time units). Since the channel transit time is known, observe that as the fluid that was at the inlet at time C reaches the channel exit shortly after F, the mixture density (at the exit), as expected, starts to increase. (In fact, throughout the cycle, variation in exit mixture density follows the variation in inlet velocity with an average delay close to the average channel transit time.) But the pressure drop at the exit is proportional to density *as well as* to the square

of the mixture velocity [3], and mixture velocity keeps decreasing even after the fluid that was at the channel inlet at time C reaches the channel exit. [This is because, although the mixture velocity in the two-phase region is proportional to the channel inlet velocity, it decreases as the boiling boundary moves up, see [13]. Actually, for large values of N_{pch}, mixture velocity is largely determined by the boiling boundary variation and hence, even when the inlet velocity is increasing, the two-phase mixture velocity continues to decrease. The two-phase mixture velocity continues to decrease even after (almost up to time H) the inlet velocity has reached its peak at time G.] Comparing the variation in exit pressure drop with variations in exit mixture velocity and exit mixture density, makes it clear that since the exit pressure drop more closely follows the former, it is clearly being influenced more by the variation in the mixture velocity than by variation in mixture density. Moreover, due to the phase lag between the maximum in exit mixture density and the maximum in exit mixture velocity, the maximum in exit pressure drop occurs between the two maxima, closer to the mixture velocity maximum—indicating the relative importance of mixture velocity variation over mixture density variation in determining the channel pressure drop characteristics, and hence, in the feedback process, see [3].

To study the role of traveling density waves, we now analyze the space- and time-dependent variation of mixture velocity and mixture density. Mixture velocity changes by the same amount at every time step throughout the two-phase region. Mixture density in the entire two-phase region increases (or decreases) almost simultaneously, and hence, there is only a weak density *wave* that travels from the lower part of the channel to the top. During approximately half the oscillation cycle, the mixture density in the two-phase region increases. At the beginning of the cycle it increases mostly near the boiling boundary and the region closer to the exit is largely unaffected. As the cycle develops *while continuing to increase near the lower portion of the two-phase region*, the mixture density also starts to increase at progressively higher elevation. The mixture density everywhere in the two-phase region reaches its maximum at almost the same time.

This numerical example shows that strong traveling density *waves* are not essential for these non-linear oscillations and that these oscillations may persist—at least in some regions of the parameter space—even when traveling density waves are fairly weak. Even when strong traveling density *waves* do appear during oscillations while operating at other regions in parameter space (see case B), their effect on channel dynamics is considerably smaller than the effect of variation in volumetric flow rate that accompanies them.

Oscillation period versus channel residence time

The oscillation period for density-wave oscillations is traditionally reported (Stenning & Veziroğlu 1965; Bouré 1978; Kakaç & Liu 1991) to be about twice the channel transit time. In this section, numerical results presented in figures 2 and 3 are used to develop a relationship between channel transit time and the oscillation period, and it is shown that the period of these oscillations is actually closer to four times the channel transit time.

For the case of spatially uniform and time-independent heat flux, single-phase residence time v, even during the oscillation, is in general, constant, while the two-phase residence time oscillates (Achard *et al.* 1985; Rizwan-uddin & Dorning 1986). For case A, single-phase residence time v is equal to 0.59 and the two-phase residence time oscillates between 0.09 and 0.15. Hence, the total transit time during the oscillation oscillates between 0.68 and 0.74. The period of oscillation is about 2.4. To identify the physical mechanism behind the relationship between the oscillation period and the channel transit time, we note that there is an unstable fixed point that corresponds to the inlet velocity of 1.0, and once again follow the fluid at the channel inlet at time C. After approximately one average channel transit time, this fluid reaches the channel exit near time E. But the information it carried with it to the channel exit—based on which the inlet velocity, through pressure feedback, is modified—is that although the inlet velocity is increasing, it is at its minimum, below the unstable steady-state value, i.e. the pressure drop at the exit near time E corresponds to the inlet velocity at C and hence, is lower than the pressure drop at the unstable fixed point. The result of the feedback is, hence, to continue increasing the inlet velocity. Since, by the time this information (inlet velocity at its minimum) reached the channel exit near time E, the inlet velocity was already close to its steady-state value, it keeps increasing beyond that value. When the fluid which is at the channel inlet at time E, after another channel average transit time, reaches the channel exit near

time G, with the information that the inlet velocity is near its steady-state value and still increasing, the pressure feedback process tries to stem the increase and, hence, the inlet velocity, after increasing for approximately two-average-channel-transit-times, starts to decrease at time G. Again, because of the delay, the exit learns at time A about the inlet velocity behavior at time G (inlet velocity above the unstable steady-state value) and, hence, forces the inlet velocity to decrease further, all the way up to time C. As is clear, this explanation actually implies the oscillation period to be close to four times the channel transit time, which is supported by the numerical results.

Possible reasons for the differences between the conclusions drawn above and the mechanism of density-wave oscillations proposed by previous authors are discussed in the next section. Also reported in the next section is the experimental evidence (Saha *et al.* 1976) supporting the relationship between the oscillation period and channel residence time suggested above.

Case B

In order to analyze the oscillation mechanism in a more realistic channel with distributed pressure drop, and to compare it with the simpler channel case, the distributed pressure drops—frictional, gravitational and accelerational—are introduced in the model. The total channel pressure drop now is the sum of inlet pressure drop, single-phase region pressure drop, two-phase region pressure drop and exit pressure drop, see [1]. Parameter values and steady-state values of the dependent variables for this case (case B) are given in table 2. Evolution of the inlet velocity, after a small perturbation at the unstable steady-state, to stable limit cycle oscillation is shown in figure 4(a). In figure 4(b) is shown the phase space trajectory in the v_i–λ plane. In figure 5(a)–(e) are shown the inlet pressure drop, exit pressure drop, single-phase region pressure drop, two-phase region pressure drop, inlet velocity, boiling boundary, mixture density and mixture velocity at four points in the two-phase region ($z = 0.7$, 0.8, 0.9, 1.0), and channel residence time over one period of the stable limit cycle oscillation. The results of case B are similar to those of case A, and they further support the conclusions drawn from the simpler case in which the distributed pressure drop was ignored.

There clearly is a traveling density wave in this numerical experiment, as can be seen in figure 5(c). But pressure drop at axial locations where the crest of the wave passes through, actually—due to an even larger simultaneous drop in mixture velocity—decreases. This again is contrary to the traditional explanations of density-wave oscillations that require the pressure drop to increase as fluid waves of higher density pass through. Hence, it is clear that at least in some regions of parameter space, traveling density waves during these non-linear oscillations, are not strong enough to increase the local pressure drop as fluid waves of higher density pass through; the simultaneous variation (reduction) in mixture velocity is actually so strong that local pressure drop decreases. Dykhuizen *et al.* (1986b), who used a two-fluid model to simulate oscillations, also found that fractional changes in vapor fraction near the channel exit (at 4.25 m, where the channel is 5.25 m long) are significantly smaller than fractional changes in velocity. Though not explicitly stated, it is clear from the numerical results presented in the paper that their simulations also showed the local pressure drop to actually increase as the wave of lower vapor fraction passes through.

Table 2

Parameters	N_{sub}	4.50
	N_{pch}	8.90
	ΔP_{ex}	45.60
	Fr^{-1}	10.00
	N_{fl}	2.80
	N_{fl}	8.4
	k_i	6.0
	k_e	2.5
Dependent variables	Inlet velocity	1.00
	Boiling boundary	0.51
	ΔP_i	6.00
	ΔP_e	13.51
	$\Delta P_{1\phi}$	6.47
	$\Delta P_{2\phi}$	10.62
	$\Delta P_{tot} (= \Delta P_{ex})$	45.60

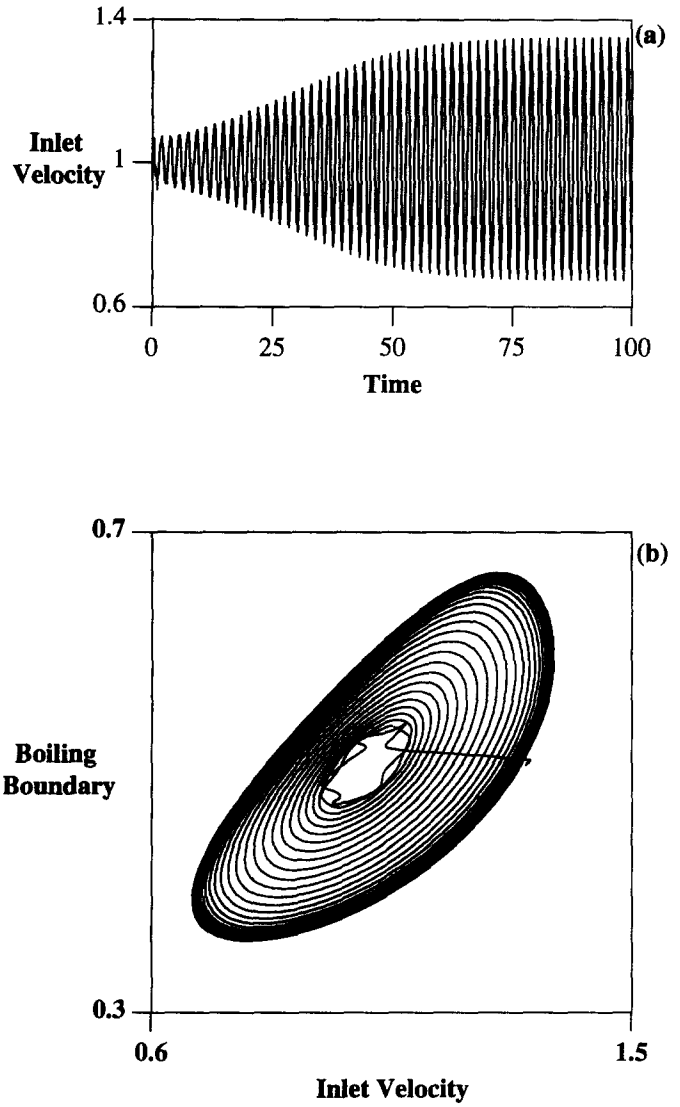

Figure 4. (a) Evolution of the inlet velocity as a function of time for case B. (b) Trajectory in a projection of the phase space onto the two-dimensional v_i–λ plane.

The oscillation mechanism described earlier for case A is also relevant to this more general case. The effect on channel dynamics of including the distributed pressure drop is that the feedback process becomes a little faster. This is because a change in inlet flow rate does not have to propagate all the way to the channel exit to affect the internal pressure drop, whereas, for the case of no distributed pressure drop in the single- and two-phase regions, an inlet velocity variation had to travel all the way to the channel exit in approximately one channel transit time, to influence the pressure drop characteristics which in turn, through the feedback process, modulated the inlet velocity. Now, with distributed pressure drop included, a variation in inlet flow rate starts affecting the single-phase region pressure drop immediately and even the two-phase region pressure drop after a delay that is obviously shorter than the delay for the exit pressure drop. Hence, when distributed pressure drop is included, the total internal pressure drop responds to changes in the inlet flow rate on a time scale shorter than the channel transit time and therefore, the oscillation period is expected to be shorter than four-channel-transit-times. Note, the oscillation period in case B is still greater than three times the average channel transit time.

The extent to which the oscillation period depends upon the channel transit time depends upon the steady-state pressure drop distribution along the channel length. If a large fraction of the total

pressure drop is concentrated near the channel exit, then the oscillation period—even in the presence of distributed pressure drop—will be closer to four times the channel transit time. On the other hand, if a significant fraction of the internal pressure drop occurs closer to the channel inlet then, of course, the feedback process responds to variations in inlet velocity sooner than channel transit time and therefore, the oscillation period is expected to be less than four-channel-transit-times.

The distribution of the fractional pressure drop along the channel length plays an important role in determining the stability of the system. Since variations in inlet velocity get amplified as they travel through the two-phase region, their (delayed) effect is strongest on pressure drop near the channel exit. To compensate for large changes in fractional pressure drop near the exit, the inlet velocity must change drastically leading to unstable system and/or large amplitude oscillations.

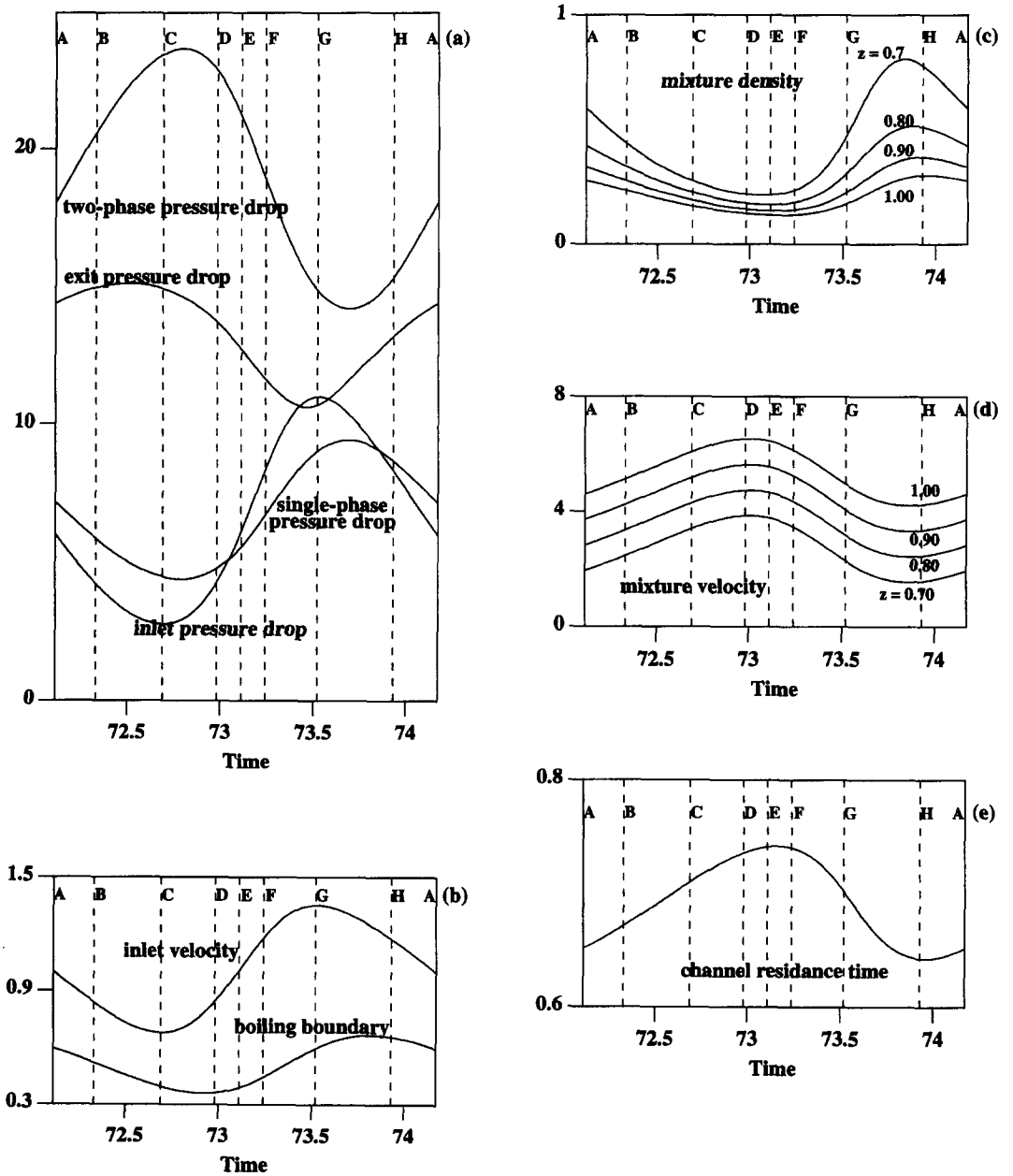

Figure 5. (a–e) Variation of the dependent variables over one period of the stable oscillation for case B. Shown are, inlet and exit pressure drop, inlet velocity, boiling boundary, mixture density and mixture velocity at four points in the two-phase region ($z = 0.7, 0.8, 0.9, 1.0$), and channel residence time ($\nu + \tau_{2\phi}$).

Hence, as has been observed in the past, a large concentration of pressure drop in the two-phase region near the channel exit leads to instability. By the same argument, a large concentrated pressure drop coefficient at the channel inlet enables the system to compensate for fractional pressure drop variation in the two-phase region by relatively small changes in inlet velocity, leading to a stable system.

To study the effect on stability of pressure drop distribution in the channel, the heated channel system for parameter values used in case B, was further analyzed. Observe that after a perturbation at time $t = 0$, the system, shown in figure 3, asymptotically evolves from the unstable fixed point to stable limit cycle oscillations. To determine the effect of lower pressure drop near the exit, the pressure drop coefficient at the exit is decreased instantly from 2.5 to 2.45 at $t = 80$, after the system has evolved to stable oscillations. The resulting transient and the new asymptotic solution are shown in figure 6(a). A decrease in the exit pressure drop coefficient leads to a smaller pressure drop at the exit and hence, a drop in the fractional pressure drop near the exit. Thus, as perturbations are propagated to the channel exit, they are not amplified as much as they were before the change in coefficient, forcing a smaller variation in the inlet velocity and resulting in smaller amplitude oscillations. In figure 6(b) is shown the inlet velocity evolution from the stable periodic solution to the stable fixed point as a result of decreasing the exit pressure drop coefficient from 2.50 to 2.40 at $t = 80$. Compared to the previous case, the fractional pressure drop near the exit in this case is decreased even further, resulting in a stable system. On the other hand, as the exit pressure drop coefficient is increased from 2.5 to 2.6 at $t = 80$, the fractional two-phase region pressure drop increases, requiring larger variation in the inlet velocity to compensate for the variation in the two-phase region pressure drop, and this results in larger amplitude oscillations. Evolution of the inlet velocity for this case is shown in figure 6(c). Clearly, in the case of the larger two-phase region pressure drop, the variation in the two-phase region pressure drop is also larger, as the inlet velocity variations are propagated downstream, requiring larger amplitude oscillations.

DISCUSSION

Cases A and B, discussed in the previous section, quite clearly demonstrate the physical mechanism behind the so-called density-wave oscillations. Two processes are fundamental to these non-linear oscillations: (1) delayed effects of inlet velocity variation on channel pressure drop characteristics; and (2) the feedback process by which the system compensates, by varying the inlet velocity at time t, for any pressure drop variation that results due to changes in inlet velocity at earlier times. A combination of these two processes leads to stable periodic oscillations of finite amplitude. The detailed process has been explained in the previous section.

The fact that the details of the physical mechanism behind the density-wave oscillations proposed here are different—sometimes even contradictory—from those proposed earlier, requires some explanation for the differences. Specifically, there are two issues: relative importance of mixture velocity versus mixture density and the role of traveling density waves; and the relationship between channel transit time and oscillation period. The issue of the relative importance of mixture density variation versus mixture velocity variation during stable oscillations is addressed first.

Some of the initial two-phase boiling flow experiments were carried out at extremely low Reynolds numbers (Stenning & Veziroğlu 1965). In such cases, the effects on local pressure drop of the mixture density variation can be more dominating or at least comparable to the effects of mixture velocity variation, and hence, an increase in mixture density, associated with the crest of a traveling density wave, would lead to an increase in local pressure drop. Since the study of Stenning & Veziroğlu (1965), even when analyzing systems with relatively large Reynolds numbers, the same mechanism has been assumed to be valid, which as clearly shown, is not the case.

The second issue is that of the relationship between oscillation period and channel transit time. The experimental set up of one of the first analyses (Stenning & Veziroğlu 1965) that reported the oscillation period to be close to the channel transit time, included a supply tank, a surge tank and a heated channel. The pressure drop was kept constant between the supply tank and the channel exit, which makes the actual system significantly larger than the heated channel alone. The actual *system* transit time (from the supply tank to the channel exit), which was not reported, must be larger than the heated channel transit time that was reported, and found to be close to the

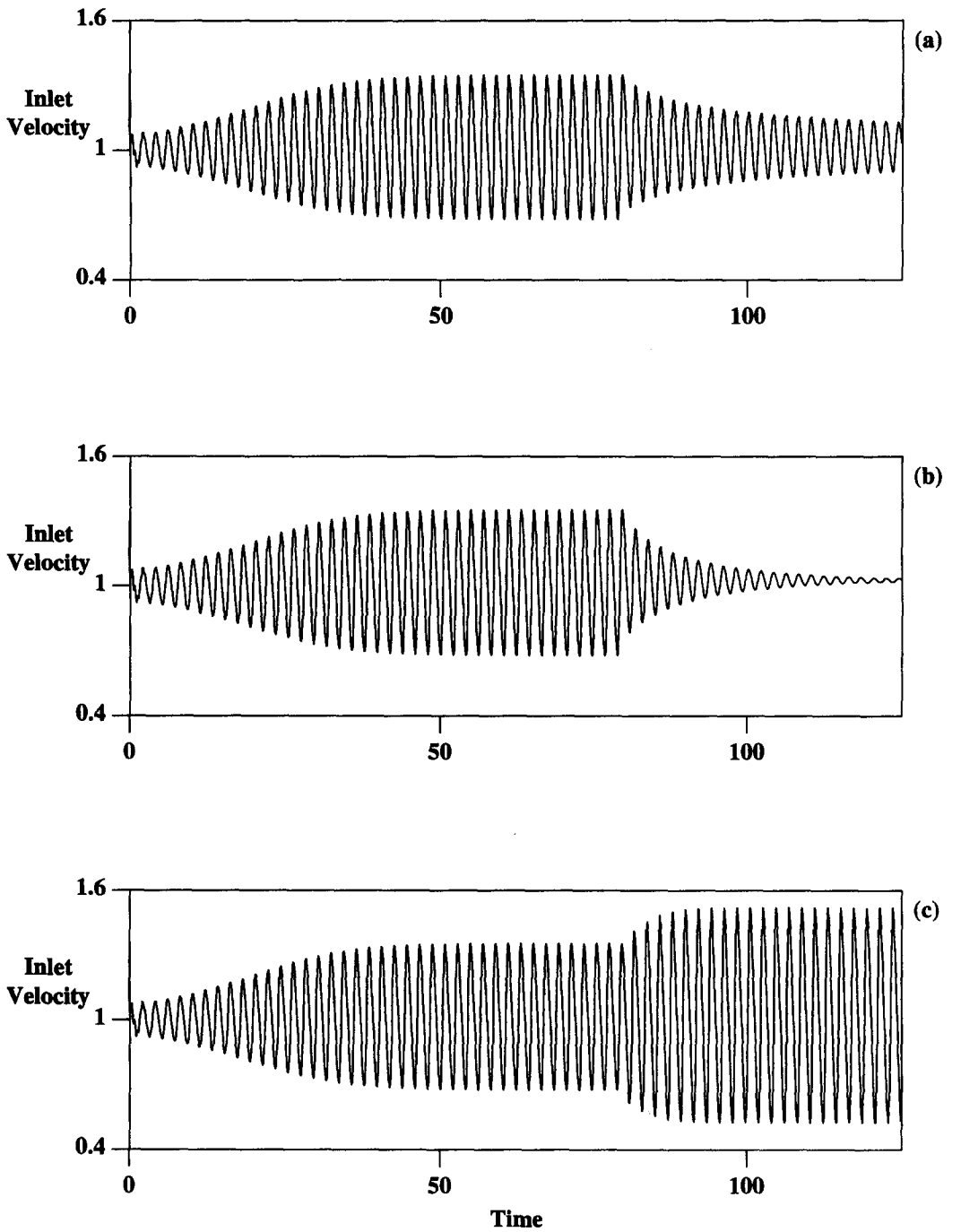

Figure 6. Effect of change in fractional pressure drop near the channel exit. (a) Decrease k_e from 2.5 to 2.45 at $t = 80$; (b) decrease k_e from 2.5 to 2.40 at $t = 80$; (c) increase k_e from 2.5 to 2.60 at $t = 80$.

oscillation period. In many experimental analyses since then, a constant pressure drop boundary condition is imposed across the heated channel by using a large parallel by-pass. In such systems, the transit time between two constant pressure points is actually just the channel transit time. Following Stenning & Veziroğlu (1965)—who correctly identified the oscillation period in their experiment to be close to the system transit time—several authors have erroneously assumed the oscillation period, even in parallel channel flow, to be close to the channel transit time. We have calculated the channel transit time from the experimental data reported by Saha *et al.* (1976)—who,

Table 3. Ratio of oscillation period and channel residence time in experimental data (Saha *et al.* 1976, Set II)

f	$T = 1/f$	Single-phase residence time $v = N_{sub}/N_{pch}$	Two-phase residence time $\tau_{2\phi}$	Channel residence time $(v + \tau_{2\phi})$	$T/[(v + \tau_{2\phi})]$
0.33	3.07	0.565	0.145	0.710	4.32
0.33	3.03	0.550	0.156	0.706	4.28
0.35	2.86	0.540	0.161	0.701	4.04
0.36	2.78	0.530	0.171	0.700	3.96
0.33	3.03	0.540	0.179	0.719	4.20
0.37	2.70	0.500	0.215	0.715	3.76
0.39	2.56	0.495	0.223	0.718	3.56
0.44	2.27	0.430	0.242	0.670	3.40
0.42	2.38	0.393	0.268	0.662	3.60
0.45	2.22	0.365	0.273	0.638	3.48

using a large by-pass, imposed a constant pressure drop boundary condition across the heated channel. In table 3 are shown the frequency and period of oscillation for the experimental data, Set II, as reported by Saha *et al.* (1976), and the average channel transit time calculated from the values of N_{sub}, N_{pch} and $\tilde{v}$. The ratio of oscillation period to average channel transit time is also shown. It is clear that the oscillation period reported is significantly larger than one-to-two-times the channel transit time.

CONCLUSIONS

The analysis presented in this paper clearly shows that past description of the physical mechanism behind the so-called density-wave oscillations needs to be supplemented. Through the analysis of the simplified problem with pressure drop concentrated at the channel inlet and channel exit, and the more realistic problem that includes distributed pressure drop along the length of the channel, it is clearly established that in certain regions of parameter space, variation in mixture velocity affects the pressure drop characteristics of the channel during the oscillation more than the variation in mixture density, and that *traveling* density waves do not appear to play an important role in such oscillations. Moreover, local pressure drop, due to the simultaneous increase in mixture velocity, actually increases as a "wave" of lower density passes.

It has also been found that the oscillation period, for a wide range of parameter values, is between three and four times the average channel transit time. Based on the numerical results obtained, and based on the analysis of competing dynamical effects during the oscillations, a consistent physical model for these non-linear oscillations is proposed.

Acknowledgements—This paper was prepared with the support of the U.S. Nuclear Regulatory Commission (NRC) under Grant No. NRC-04-90-113. The opinions, findings, conclusions and recommendations expressed herein are those of the authors and do not necessarily reflect the views of the NRC.

REFERENCES

ACHARD, J-L., DREW, D. A. & LAHEY, R. T., JR 1985 The analysis of nonlinear oscillations in boiling channels. *J. Fluid Mech.* **155,** 213–232.

BERGLES, A. E. 1981 Instabilities in two-phase systems. In *Two-phase Flow and Heat Transfer in the Power and Process Industries* (Edited by BERGLES, A. E., COLLIER, J. G., DELHAYE, J. M., HEWITT, J. F. & MAYINGER, F.). Hemisphere, Washington, DC.

BOURÉ, J. A. 1978 Oscillatory two-phase flows. In *Two-phase Flows and Heat Transfer with Application to Nuclear Reactor Design Problems* (Edited by GINOUX, J. J.) Hemisphere, Washington, DC.

BOURÉ, J. A., BERGLES, A. E. & TONG, L. S. 1973 Review of two-phase flow instability. *Nucl. Engng Design* **25,** 165–192.

DYKHUIZEN, R. C., ROY, R. P. & KALRA, S. P. 1986a A linear two-fluid model analysis of dynamic instability in boiling flow systems. *J. Heat Transfer* **108,** 100–108.

DYKHUIZEN, R. C., ROY, R. P. & KALRA, S. P. 1986b Two-fluid model simulation of density-wave oscillations in a boiling flow system. *Nucl. Sci. Engng* **94,** 167–179.

FRIEDLY, J. C. & KRISHNAN, V. S. 1972 Predictions of nonlinear flow oscillations in boiling channels. *AIChE Symp. Ser.* **68,** 127–135.

FRUTERA, M. 1986 Validity of homogeneous flow model for instability analysis. *Nucl. Engng Design* **95,** 65–77.

HASSARD, B. D., KAZARINOFF, N. D. & WAN, Y-H. 1981 Theory and applications of Hopf bifurcation. London Math. Soc. Lecture Note Series 41, Cambridge University Press.

HOPF, E. 1942 Abzweigung einer periodischen Losung von einer stationaren Losung eines Differentialsystems. *Ber. Verh. Sachs. Akad. Wiss. Leipsig Math.—Nat. 94.* Translation into English with commentary by HOWARD, L. & KOPELL, N.. In MARSDEN, J. E. & MCCRACKEN, M. 1976 *The Hopf Bifurcation and Its Applications*, Applid Math. Sciences, Vol. 19. Springer, New York.

KAKAÇ, S. & LIU, H. T. 1991 Two-phase flow dynamics instabilities in boiling systems. In *Multiphase Flow and Heat Transfer—Second International Symposium* (Edited by XUE-JUN CHEN, VEZIROĜLU, T. N. & TIEN, C. L.), Vol. 1, pp. 403–444. Hemisphere, Washington, DC.

LAHEY, R. T., JR, & MOODY, F. J. 1977 *The Thermal-hydraulics of a Boiling Water Nuclear Reactor.* American Nuclear Society, LaGrange Park, IL.

RIZWAN-UDDIN 1986 Nonlinear dynamics of two-phase flow. *Trans. Am. Nucl. Soc.* **53,** 238.

RIZWAN-UDDIN & DORNING, J. J. 1986 Some nonlinear dynamics of a heated channel. *Nucl. Engng Design* **93,** 1–14.

RIZWAN-UDDIN & DORNING, J. J. 1988 A chaotic attractor in a periodically forced two-phase flow system. *Nucl. Sci. Engng* **100,** 393–404; see also RIZWAN-UDDIN & DORNING, J. 1990 Chaotic dynamics of a triply-forced two-phase flow system. *Nucl. Sci. Engng* **105,** 123–135.

SAHA, P., ISHII, M. & ZUBER, N. 1976 An experimental investigation of thermally induced flow oscillations in two phase systems. *J. Heat Transfer* **98,** 616–622.

STENNING, A. H. & VEZIROĜLU, T. N. 1965 Flow oscillations modes in forced convection boiling. *Proc. 1965 Heat Transfer and Fluid Mech. Inst.*, pp. 301–316. Stanford University Press, CA.

APPENDIX

The Dimensionless Variables and Parameters

The single- and two-phase region equations are made dimensionless using the dimensional channel length L^*, liquid density ρ_f^*, latent heat Δh_{fg}^* and an arbitrary characteristic velocity v_0^*. The dimensionless variables and parameters that appear in these equations are defined as follows:

$$j = \frac{j^*}{v_0^*}, \quad v_i = \frac{v_i^*}{v_0^*}, \quad z = \frac{z^*}{L^*},$$

$$\lambda = \frac{\lambda^*}{L^*}, \quad t = \frac{t^*}{L^*/v_0^*}, \quad \rho_m = \frac{\rho_m^*}{\rho_f^*},$$

$$h_m = \frac{h_m^*}{\Delta h_{fG}^*}, \quad P = \frac{P^*}{\rho_f^* v_0^{*2}}, \quad \mathrm{Fr} = \frac{v_0^{*2}}{g^* L^*},$$

$$N_\rho = \frac{\rho_G^*}{\rho_f^*}, \quad N_r = \frac{\rho_f^*}{\Delta\rho^*}, \quad N_\rho = 1 - \frac{1}{N_r},$$

$$N_{fl} = \frac{f_s^* L^*}{2D^*}, \quad N_{f2} = \frac{f_m^* L^*}{2D^*}, \quad N_{sub} = \frac{\Delta h_f^* \Delta\rho^*}{\Delta h_{fG}^* \rho_G^*},$$

$$N_{pch} = \frac{q''^* \xi^* L \Delta\rho^*}{A^* \Delta h_{fG}^* \rho_G^* \rho_f^* v_0^*}$$